# Performance Analysis and Cross Layer Optimization for Multimedia Streaming over Wireless Networks

Antonio Ao, Zhung-Han Wu, and Ping-Cheng Yeh

Graduate Institute of Communication Engineering,
National Taiwan University, Taipei, Taiwan
{r96942044,f97942031,pcyeh}@ntu.edu.tw

**Abstract.** Multimedia data are sensitive to delay which deteriorates the video quality and the perception of the viewer. Due to the sensitivity to the delay, transmitting multimedia data over inherently variant wireless channels is a big challenge. Although wireless systems have employed adaptive modulation and coding (AMC) to combat the variation of the environment, the possible delay in the buffers still has impacts on the video quality. In this paper, the focus is on the performance of wireless multimedia streaming using AMC. In particular, the video frame error rate and the resulting GOP distortion for video streaming is analyzed. It is observed that the video quality depends on the target packet error rate of the AMC, which also determines the SNR thresholds of AMC. Through our analysis, the optimal target PER of AMC and the resulting SNR thresholds can be obtained to achieve the optimal video quality that minimizes the GOP distortion.

**Keywords:** queueing analysis, cross layer optimization, multimedia, streaming, AMC, distortion.

## 1 Introduction

Multimedia streaming faces a big challenge in delivering multimedia data within strict delay bound for the receiving node to reconstruct the video streaming in time. On the other hand, the nature of the varying wireless channels results in even bigger challenge for wireless multimedia streaming. Different techniques have been proposed to deal with the varying channels. Adaptive modulation and coding (AMC) is a technique commonly used which dynamically adjusts the modulation and coding according to the channel condition to maximize the overall throughput. When multimedia streaming application is performed upon wireless networks with AMC, the video quality is significantly affected by AMC. When the channel condition is bad, AMC transmits data with low rate mode to ensure low probability of error during the transmission. Yet, there is a tradeoff here. Due to the low transmission rate of AMC under the poor channel state, the data packets may be queued in the buffer and experience longer delays due to bad channel conditions. Under such circumstances, the delay sensitive multimedia packets may be dropped due to timeouts and buffer overflows. The dropped packets thus cause severe deterioration to the quality of the reconstructed video.

In the literature, several works explore the effect of AMC on the queueing behavior of wireless transmissions. The first study analyzing the queueing behavior of wireless

N. Bartolini et al. (Eds.): QShine/AAA-IDEA 2009, LNICST 22, pp. 647–662, 2009.

transmissions with AMC is given in [1]. The queueing analysis is extended for AMC with automatic repeat request (ARQ) incorporated [2]. In [3], the queueing analysis with AMC over MIMO system is studied. It is noted that the works in [1, 2, 3] do not consider the timeout problem of delay-sensitive traffic when transmitting with AMC. There have been some works focusing on the issue. In [4], the authors consider the problem of scalable video transmission with adaptive BCH codes. However, BCH codes are not commonly used in practical AMC. In [5, 6], the timeout probability of video traffic over AMC transmission is analyzed using the effective capacity method. The quality of the reconstructed video and the effect of cross traffic from other multimedia streams are not considered in these works.

In this paper, a cross-layer optimization algorithm for maximizing video quality is proposed. The queue of multimedia streaming via AMC is first analyzed. The analysis is then applied to analyze the video frame error rate (VFER) and the resulting GOP distortion for the video streaming. The effect of the interruption of cross traffic from other multimedia streams is also analyzed. It is observed that the video quality depends on the target packet error rate (PER) of AMC, which also determines the SNR thresholds of AMC. Through our analysis, the optimal target PER of AMC and the resulting SNR thresholds can be obtained to achieve the optimal video quality that minimizes the GOP distortion.

The remainder of the paper is organized as follows. In Section 2, the system model is first described. In Section 3, we analyze the video streaming quality for the case of single multimedia stream. In Section 4, we extend the work to the case of multiple streams. The analysis in these sections enables us to determine the optimal AMC for video streaming. In Section 5, the numerical results are presented. Finally, the conclusions are given in Section 6.

## 2 System Model

### 2.1 System Description

The block diagram of wireless multimedia transmission from a base station to a mobile receiver through fading channels is illustrated in Figure 1. At the base station, a classifier divides the arriving packet into two categories, delay sensitive multimedia packets and delay insensitive data packets. The two classes of packets are sent to two different buffers, the media buffer and the data buffer respectively. In this work, we consider a general model which allows the base station to serve multiple multimedia streams at the same time. At the mobile receiver, it estimates the channel quality to decide the AMC mode to use. The AMC mode choice is then fed back to base station for the PHY mode controller to adjust the modulation/coding for packet transmissions.

### 2.2 Packet/MAC Frame Structure

Real-time multimedia packet transmissions employ UDP protocol to avoid the extra delay caused by retransmissions. As shown in Figure 2, a UDP packet contains header, payload and CRC. The packet accommodates $N_b$ = 11680 bits (1460 bytes). The CRC

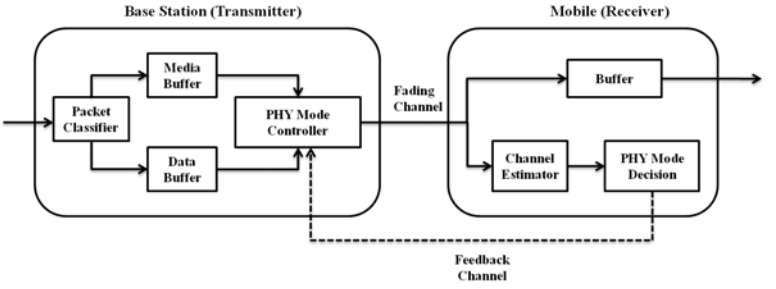


**Fig. 1.** Wireless multimedia transmissions via AMC

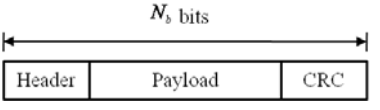


**Fig. 2.** Packet structure

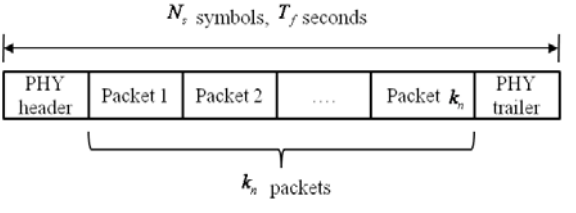


**Fig. 3.** MAC frame structure

is assumed perfect for packet error detection. If a packet is detected to be in error, the packet is dropped and declared packet loss. The header and the CRC parity bits are assumed to be negligible for throughput calculation.

Fig. 3 illustrates the MAC frame structure. Each MAC frame consists of header, trailer and packets coming from upper layer. Each MAC frame contains $N_s$ symbols and the MAC frame duration is $T_f$ seconds. Given the AMC mode is in mode $n$ with transmission rate $R_n$, the value of $N_s$ can be calculated by

$$N_s = N_{overhead} + \frac{k_n N_b}{R_n} \approx \frac{k_n N_b}{R_n}, \tag{1}$$

where $k_n$ is the number of packets in a MAC frame, and $N_{overhead}$ denotes the number of symbols of physical layer overhead. Note that $N_{overhead}$ can be ignored because it is much less relative to the number of payload symbols. Thus

$$k_n \approx \frac{N_s}{N_b} R_n = bR_n \tag{2}$$

where $b \triangleq N_s/N_b$. $b$ is the number of total packets grouped together per MAC frame given rate $R_n$.

### 2.3 AMC Transmission Modes and Packet Error Rate

In this paper, the following transmission mode (TM) for physical layer AMC is considered. The transmission modes use $M_n$ QAM modulation with punctured convolutional codes. Monte Carlo simulation is conducted to obtain the exact PER. The simulation block diagram is depicted in Figure 4. The generator polynomial of mother code is $g$ = [133, 171], and the coding rate and puncturing pattern are adopted from IEEE 802.11a [7]. The packet size is set to be the same as $N_b$ (1460 bytes). For the sake of analysis, the simulated PER of each AMC mode $n$ is fitted by a piecewise function $p_n(\gamma)$ as

$$p_n(\gamma) = \begin{cases} 1, & \text{if } \gamma < \gamma_{pn} \\ \exp(a_n - g_n\gamma), & \text{if } \gamma \geq \gamma_{pn}, \end{cases} \tag{3}$$

Simulation and fitting results are shown in Figure 5. The figure shows the fitting curves well match the simulation curves. In Table 1 we summarize the fitting results of each transmission mode.

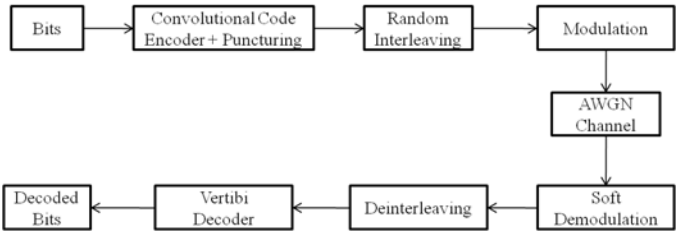


**Fig. 4.** Block diagram of TM simulation

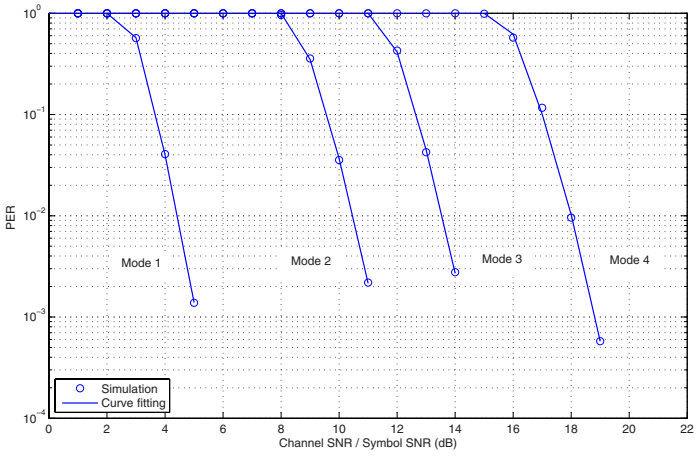


**Fig. 5.** Packet error rate versus channel SNR in different modes, packet size = 1460 bytes

**Table 1.** Curve fitting parameters in different modes

| | Mode 0 | Mode 1 | Mode 2 | Mode 3 | Mode 4 |
|---|---|---|---|---|---|
| Modulation | - | QPSK | 16-QAM | 16-QAM | 64-QAM |
| Coding Rate $R_c$ | - | 1/2 | 1/2 | 3/4 | 2/3 |
| $R_n$ (bits/sym.) | 0 | 1 | 2 | 3 | 4 |
| $a_n$ | - | 9.7413 | 7.6572 | 7.7266 | 6.5429 |
| $g_n$ | - | 5.1606 | 1.0960 | 0.5430 | 0.1022 |
| $\gamma_{pn}$(dB) | - | 3 | 9 | 12 | 16 |

### 2.4 FSMC Wireless Channel Model

FSMC is widely used to model the varying wireless channel which matches well with the actual channel measurement experiments. The channel SNR is partitioned into $N+1$ non-overlapping consecutive intervals by the SNR threshold points $\{\gamma_n\}_{n=0}^{N+1}$, and each SNR interval is associated with an AMC mode. When the received channel SNR $\gamma$ falls in $[\gamma_n, \gamma_{n+1})$, the channel is said to be in channel state $n$ and AMC mode $n$ is used for transmission. The SNR thresholds $\{\gamma_n\}_{n=0}^{N+1}$ are determined by the QoS criteria in the following section. Based on [9] and [10], the probability of the channel being in state $n$ is

$$\begin{aligned}\Pr(n) &= \int_{\gamma_n}^{\gamma_{n+1}} p(\gamma)d\gamma \\ &= \frac{\Gamma(m, \frac{m\gamma_n}{\overline{\gamma}}) - \Gamma(m, \frac{m\gamma_{n+1}}{\overline{\gamma}})}{\Gamma(m)},\end{aligned} \tag{4}$$

where

$$\Gamma(m, x) = \int_x^{\infty} t^{m-1} \exp(-t)dt$$

is the complementary incomplete Gamma function, and

$$p(\gamma) = \frac{m^m \gamma^{m-1}}{\overline{\gamma}^m \Gamma(m)} \exp(-\frac{m\gamma}{\overline{\gamma}}) \tag{5}$$

is the probability density function (pdf) of the commonly used Nakagami-$m$ distribution for modeling the receive channel SNR. Note that $\overline{\gamma} = E\{\gamma\}$ denotes the average received SNR and $\Gamma(m) = \int_0^{\infty} t^{m-1} \exp(-t)dt$ is the Gamma function.

Since the channel is varying continuously, it is generally assumed that the channel state transition probability $P_{m,n} = 0$ for any nonconsecutive states $m, n$ such that $|m - n| \geqslant 2$. The remaining nonzero transition probabilities are the adjacent-state transition probabilities which can be computed as [11]

$$\begin{aligned}P_{n,n+1} &= \frac{N_{n+1}T_f}{\Pr(n)}, \text{if } n = 0, 1, ..., N-1 \ . \\ P_{n,n-1} &= \frac{N_n T_f}{\Pr(n)} \quad , \text{if } n = 1, ..., N,\end{aligned} \tag{6}$$

where $N_n$ denotes the level crossing rate of state $n$. The value of $N_n$ can be approximated by [12]

$$N_n = \frac{\sqrt{2}\pi f_d}{\Gamma(m)}(\frac{m\gamma_n}{\overline{\gamma}})^{m-0.5}exp(-\frac{m\gamma_n}{\overline{\gamma}}), \tag{7}$$

where $f_d$ denotes the maximum Doppler shift. The $(N+1)\times(N+1)$ channel state transition probability matrix $P_c$ can then be expressed as

$$\mathbf{P}_c = \begin{bmatrix} 1-P_{0,1} & P_{0,1} & \cdots & 0 \\ P_{1,0} & 1-P_{1,0}-P_{1,2} & P_{1,2} & \vdots \\ 0 & \ddots & \ddots & 0 \\ \vdots & P_{N-1,N-2} & 1-P_{N-1,N-2}-P_{N-1,N} & P_{N-1,N} \\ 0 & \cdots & P_{N,N-1} & 1-P_{N,N-1} \end{bmatrix}. \tag{8}$$

### 2.5 QoS Criteria and AMC SNR Thresholds

In this paper, we consider the QoS criteria which requires the target average PER of the AMC, $\overline{\text{PER}}$, to be $P_0$. The average PER of AMC in mode $n$ is of the form [10]

$$\begin{aligned} \overline{\text{PER}}_n &= \frac{1}{\text{Pr}(n)}\int_{\gamma_n}^{\gamma_{n+1}} \exp(a_n - g_n\gamma)p(\gamma)d\gamma \\ &= \frac{1}{\text{Pr}(n)}\frac{\exp(a_n)}{\Gamma(m)}\left(\frac{m}{\overline{\gamma}}\right)^m \frac{\Gamma(m,b_n\gamma_n)-\Gamma(m,b_n\gamma_{n+1})}{(b_n)^m} \\ &\quad ,n=1,...,N, \end{aligned} \tag{9}$$

where

$$b_n = \frac{m}{\overline{\gamma}} + g_n. \tag{10}$$

The average PER of AMC can then be obtained as the ratio of the average number of error packets over the total average number of transmitted packets. Together with the QoS criteria, we have the following equation

$$\overline{\text{PER}} = \frac{\sum_{n=1}^{N} R_n \text{Pr}(n)\overline{\text{PER}}_n}{\sum_{n=1}^{N} R_n \text{Pr}(n)} = P_0. \tag{11}$$

One can find the AMC SNR thresholds $\{\gamma_n\}_{n=0}^{N+1}$ from the equation above following the algorithm in [1], which we omit the details here.

### 2.6 Queueing Model

Detailed description of the queueing model is given as follows.

**Queueing Policy.** The media buffer and the data buffer are both of finite buffer lengths. The time is divided into slots, each of length equal to MAC frame duration $T_f$. Each

buffer operates following the first-come first-serve (FCFS) policy. When the buffer is full, the newly arrived packets are dropped. Each packet in the queue waits for at most $P$ time slots for service before it gets timeout and discarded. There is no retransmission when multimedia packet transmission error occurs so as not to introduce extra delay. Throughout the paper, it is assumed that the media buffer has higher priority over the data buffer. The data packets are served only when the media server is empty. Thus the focus is on analyzing the performance of the media queue in this paper.

**Arrival Process.** For the media queue, it is assumed that the aggregated packet arrival from multiple multimedia streams is a Poisson process with mean $\lambda T_f$. The probability mass function of the number of arrival is

$$P(A=k)=\begin{cases}\dfrac{(\lambda T_f)^k \exp(-\lambda T_f)}{k!}, & \text{if } k \geq 0\\ 0, & \text{else,}\end{cases} \tag{12}$$

where $A \in \{0,1,2,...\}$. In the case of multiple multimedia streams, we assume the video packets of each multimedia stream arrive in a batch during each slot due to the packet aggregation of the stream in the previous hop. This indicates that in each slot, packets from certain stream A either all arrive before or all arrive after the packet batch of another stream B. It is assumed that there are no interlacing of packets from two different multimedia streams within each slot.

**Service Policy.** The service rate of the queue dynamically adjusts according to the channel state and the associated AMC mode. When the FSMC state is $n$, the AMC is in mode $n$ which transmits $c_n$ packets per time slot. From (2), it is noted that $c_n = k_n = bR_n$. The set of all possible service rates is denoted by $\Psi = \{c_0, c_1, ..., c_N\}$. At the beginning of the slot, the server discards the time-out packets which have waited for $P$ time-units. The server sends packets out of the queue at the beginning of the slot based on the service rate $c \in \Psi$ of the slot. It is also noted that the packet arrivals within each slot can not be served until the next slot.

## 3 Performance Analysis for Single Stream Case

In this Section, the queue is studied for the case of single multimedia stream. In particular, we induce a refined Markov chain from the queue. The state of the refined Markov chain specifies the current service rate resulted from AMC, and the delays experienced by the current packets in the queue. The transition probabilities of the refined Markov chain is derived and it enables us to find the steady state probability of the refined Markov chain. The steady state probability is further used for analyzing the video quality of the multimedia stream.

### 3.1 Refined Markov Chain

Let $S_{(c,u_1,...,u_P)}$ denote the state of the refined Markov chain induced from the media queue, where $c \in \Psi$ denotes the service rate of the server at the time and $u_i$ denotes

the number of packets having waited $i$ time slots in the queue. In particular, $u_P$ denotes the number of packets having waited $P$ time slots and thus exceeded their lifetimes. Since the media buffer is of finite length $K$, we can express the space of all valid $\underline{u} = (u_1, ..., u_P)$ as

$$\underline{u} \in \Omega, \quad \Omega = \left\{ (u_1, u_2, ..., u_P) \left| \begin{array}{l} u_i \in \{0, 1, ..., K\}, i = 1, ..., P \\ \text{and } u_1 + u_2 + ... + u_P \leq K \end{array} \right. \right\}. \tag{13}$$

For the sake of clarity, we also use the notation of $S_{(c,\underline{u})}$ to denote $S_{(c,u_1,...,u_P)}$ throughout our work. The total number of states for the refined Markov chain can be is

$$L = (N+1) \sum_{n=0}^{K} H_n^P = (N+1) \sum_{n=0}^{K} \frac{(P+n-1)!}{(P-1)!n!}. \tag{14}$$

Based on the queueing model in Section 2.6, one can observe that for the refined Markov chain of current slot to transit from $S_{(c,\underline{u})} = S_{(c,u_1,...,u_P)}$ to $S_{(d,\underline{v})} = S_{(d,v_1,...,v_P)}$ in the next slot, where $(c, \underline{u})$ and $(d, \underline{v})$ must satisfy the the following constraints:

1. For the element $v_P$,
$$v_P = \max\{0, u_{P-1} - c\}. \tag{15}$$
2. For the $v_{P-n}$ term, where $1 \leqslant n < P - 1$,
$$v_{P-n} = \begin{cases} \max\{0, \sum_{j=1}^{n+1} v_{P-j} - c\}, & \text{if } v_{P-n+1} = 0 \\ u_{P-n-1}, & \text{if } v_{P-n+1} \neq 0. \end{cases} \tag{16}$$
3. Given the current state of the refine Markov chain is $S_{(c,\underline{u})}$, the number of packets remaining in the queue within after the packet transmissions of the current slot is
$$L_{(c,\underline{u})} = \max\{0, \sum_{j=1}^{P-1} u_j - c\}, \tag{17}$$
and the number of free space in the queue is
$$F_{(c,\underline{u})} = K - L_{(c,\underline{u})} = K - \max\{0, \sum_{j=1}^{P-1} u_j - c\}. \tag{18}$$
If there are total of $A$ packets arriving during the slot, it is obvious to see that $v_1$ satisfies
$$v_1 = \begin{cases} A, & \text{if } A < F_{(c,\underline{u})} \\ F_{(c,\underline{u})}, & \text{if } A \geq F_{(c,\underline{u})}. \end{cases} \tag{19}$$

From the constraints above, we can derive the $L \times L$ transition probability matrix of the refined Markov chain. Define the transition probability matrix as

$$\mathbf{P} = \left[ P_{(c,\underline{u}),(d,\underline{v})} \right], \tag{20}$$

where $P_{(c,\underline{u}),(d,\underline{v})}$ denotes the transition probability from $S_{(c,\underline{u})}$ to $S_{(d,\underline{v})}$, $c, d \in \Psi$ and $\underline{u}, \underline{v} \in \Omega$. The transition probability depends on the service rate transition, arrival

process, and waiting times experience by the current packets in the queue. It can be derived as

$$P_{(c,d),(\underline{u},\underline{v})} = P(S_{(d,\underline{v})}|S_{(c,\underline{u})}) = P(d|c)P(\underline{v}|S_{(c,\underline{u})}) = P_{c,d}P(\underline{v}|S_{(c,\underline{u})}), \tag{21}$$

where $P_{c,d}$ is the transition probability of the service rate. Note that the service rate transition is determined by the FSMC state transition. If $c = c_m$ and $d = d_n$, $P_{c,d} = P_{c_m,d_n} = P_{mn}$ of matrix $\mathbf{P}_c$ in (8). On the other hand, for $P(\underline{v}|S_{(c,\underline{u})})$, it is easy to see $P(\underline{v}|S_{(c,\underline{u})}) = 0$ if $c$, $\underline{u}$ $\underline{v}$ do not satisfy the constraints (15),(16). Thus we have

$$P(\underline{v}|S_{(c,\underline{u})}) = \begin{cases} P(v_1|S_{(c,\underline{u})}), & \text{if } \underline{v},\ c \text{ and } \underline{u} \text{ satisfy (15) ,(16)} \\ 0, & \text{else,} \end{cases} \tag{22}$$

with

$$P(v_1|S_{(c,\underline{u})}) = \begin{cases} P(A = v_1), & v_1 < F_{(c,\underline{u})} \\ 1 - \sum_{k=0}^{F_{(c,\underline{u})}} P(A = k), & v_1 \geq F_{(c,\underline{u})} \end{cases}. \tag{23}$$

Through (21)-(23), one can obtain $\mathbf{P}$ in (20). Denote the steady state probability of the refined Markov chain at state $S_{(c,\underline{u})}$ by $\pi_{(c,\underline{u})}$. Since matrix $\mathbf{P}$ is irreducible, The steady state vector $\underline{\pi} = [\pi_{(c,\underline{u})}]$ satisfies

$$\underline{\pi} = \underline{\pi}\mathbf{P}, \quad \sum_{c \in \Psi, \underline{u} \in \Omega} \pi_{(c,\underline{u})} = 1. \tag{24}$$

One can easily solve for $\underline{\pi}$ numerically.

### 3.2 Video Frame Error Rate Analysis

In MPEG video compression, the video sequence is divided into group of picture (GOP) for data compression. In each GOP, the video codec generates different types of frames, i.e. I-frame, P-frame and B-frame. The size of I-frame is generally larger than that of P-frame and B-frame. Due to varying length of the video frame, the VFER is different for different type of frames, which is a big challenge.

Assuming that the length of the video frame considered is fragmented into $N_v$ packets for transmission. We assume that these $N_v$ packets arrive the base station within one time slot. There are three possible events that causes the video frame to be in error at the receiver.

1. Blocking event $\mathcal{B}$: Any of the $N_v$ packets fails to enter the media queue when the buffer is full.
2. Timeout event $\mathcal{T}$: Any of the $N_v$ packets gets discarded due to waiting for $P$ slots in the queue.
3. PHY transmission error event $\mathcal{E}$: Any of the $N_v$ packets experiences transmission error when transmitted by AMC.

Define $P_{\mathcal{B}} = P(\mathcal{B})$, $P_{\mathcal{T}} = P(\mathcal{T})$, and $P_{\mathcal{E}} = P(\mathcal{E})$. These probabilities are derived as follows.

**Blocking Probability.** From the steady state probability $\underline{\pi}$ of the refined Markov chain, we can derive $P_{\mathcal{B}}$ as

$$P_{\mathcal{B}} = \sum_{c\in\Psi,\underline{u}\in\Omega} P(\mathcal{B}|S_{(c,\underline{u})})\pi_{(c,\underline{u})}, \tag{25}$$

where $P(\mathcal{B}|S_{(c,\underline{u})})$ is the probability of frame error due to blocking packets given $S_{(c,\underline{u})}$. The probability can be expressed as

$$\begin{aligned} P(\mathcal{B}|S_{(c,\underline{u})}) &= P\{0, F_{(c,\underline{u})} - N_v < 0\} \\ &= \begin{cases} 1, & \sum_{i=1}^{P-1} u_i - c - N_v < 0 \\ 0, & \text{otherwise.} \end{cases} \end{aligned} \tag{26}$$

**Timeout Probability.** The timeout probability can also be derived from $\underline{\pi}$ as

$$P_{\mathcal{T}} = \sum_{c\in\Psi,\underline{u}\in\Omega'_c} P(\mathcal{T}|S_{(c,\underline{u})})\pi_{(c,\underline{u})}, \tag{27}$$

where

$$\Omega'_c = \left\{ [x_1, x_2, ..., x_P] \,\middle|\, \begin{matrix} x_i \geq 0, x1 + x_2 + ... + x_P \leq K, \\ x_1 + x_2 + ... + x_{P-1} - c \geq N_v \end{matrix} \right\} \tag{28}$$

is the set of possible $\underline{u}$ which ensures that the blocking event will not occur given the current service rate $c$. Let $d_1$, $d_2$, ..., $d_{P-1}$ be the service rates in following $(P-1)$ time slots. Note that a necessary condition for any of the $N_v$ packets to be timeout is

$$d_1 + d_2 + ... + d_{P-1} < L_{(c,\underline{u})} + N_v = \max\{0, \sum_{j=1}^{P-1} u_j - c\} + N_v = I_{(c,\underline{u})}, \tag{29}$$

i.e. the total amount of the served packets in the next following $P-1$ time slots is less than the current queue length plus $N_v$. This is not a sufficient condition since it is possible to have packets in $L_{(c,\underline{u})}$ to get timeout which saves the $N_v$ packets from time out even if the inequality does not hold. The probability of the necessary condition is an upper bound of $P(\mathcal{T}|S_{(c,\underline{u})})$. We use it as an approximation of $P(\mathcal{T}|S_{(c,\underline{u})})$, which can be computed as

$$P(\mathcal{T}|S_{(c,\underline{u})}) \lessapprox \sum_{d_1+d_2+...+d_{P-1}<I_{(c,\underline{u})}} P_{c,d_1} P_{d_1,d_2} \cdots P_{d_{P-2},d_{P-1}}, \tag{30}$$

where $\{P_{d_i,d_k}\}$ is the FSMC transition probabilities from $\mathbf{P}_c$ in (8).

**PHY Transmission Error Probability.** Given that the QoS criteria demands the AMC to maintain a target PER of $P_0$, $P_{\mathcal{E}}$ can simply derived as

$$P_{\mathcal{E}} = \sum_{c\in\Psi,\underline{u}\in\Omega'_c} \{1-(1-P_0)^{N_v}\}\{1 - P(\mathcal{T}|S_{(c,\underline{u})})\}\pi_{(c,\underline{u})}. \tag{31}$$

With the three probabilities, one can see that the VFER of video frames of size $N_v$ packets is a function of $N_v$ and $P_0$, which can be expressed as

$$\begin{aligned} \xi(N_v, P_0) &= P_{\mathcal{B}} + (1-P_{\mathcal{B}})P_{\mathcal{T}} + (1-P_{\mathcal{B}})(1-P_{\mathcal{T}})P_{\mathcal{E}} \\ &= 1 - (1-P_{\mathcal{B}})(1-P_{\mathcal{T}})(1-P_{\mathcal{E}}). \end{aligned} \tag{32}$$

### 3.3 Video Codec Performance Analysis and Optimization

The performance of a video codec is often evaluated by the GOP distortion [13] and the peak signal-to-noise ratio (PSNR). Given the target error rate $P_0$ of the AMC, the expected GOP distortion can be computed as

$$D_{GOP}(P_0) = D_0 - \sum_l \triangle D_l \prod_{l' \preceq l} (1 - \xi_l(P_0)), \tag{33}$$

where $D_0$ is the expected distortion if no video frame from the GOP is received, $\triangle D_l$ is the expected distortion reduction if the $l$-th frame of the GOP is correctly received (given the previous $(l-1)$ frames are all correctly received). The model assumes that given any of the frame prior to the $l$-th frame is corrupted, the content embedded in the $l$-th frame is not decodable. The values of $D_0$ and $\triangle D_l$ are codec and content dependent. One can obtain these values simply from simulation. The VFER $\xi_l(P_0)$ is the error rate for the $l$-th frame in the GOP. Depending on the frame type of the $l$-th frame (I, P, or B) and the video content, one can find the average length $N_{v_l}$ of the $l$-th frame in the GOP via simulation. From the VFER analysis in the previous section, we can compute $\xi_l$ as

$$\xi_l(P_0) = \xi(N_{v_l}, P_0). \tag{34}$$

From the GOP distortion, we can compute the PSNR $\Gamma(P_0)$ as

$$\Gamma(P_0) = 10 \log_{10} \left( \frac{255^2}{D_{GOP}(P_0)} \right) \quad (dB). \tag{35}$$

One can see that the GOP distortion and the PSNR is a function of $P_0$. The AMC can be optimized for the video streaming performance by finding the optimal target PER $P_0^*$ that maximizes $\Gamma(P_0)$, and then determine the SNR thresholds of the AMC from $P_0^*$ following the algorithm in [1].

## 4 Performance Analysis for Multiple Streams Case

For the case of multiple multimedia streams, the cross traffic from other multimedia streams arriving the media queue earlier than the packet arrivals of the concerned stream has to be considered. In Figure 6, the arrivals from the cross traffic and the concerned

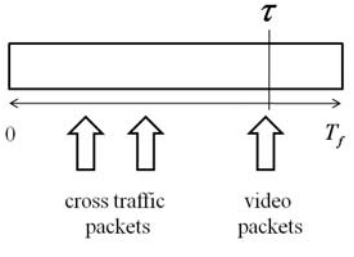


**Fig. 6.** Cross traffic arrival

video streams are depicted for the duration of a slot. Denote the arrival rate of the cross traffic by $\lambda'$ and the arrival time of the video packet batch from the concerned stream by $\tau$. Due to the property of Poisson arrival process, $\tau$ is of uniform distribution $U(0, T_f)$. The probability having $\alpha$ cross traffic packets arrival ahead of the video packets from the concerned stream can be derived as

$$\begin{aligned} P(A_c = \alpha) &= \int_0^{T_f} P\{\lambda'\tau = \alpha\} \cdot \frac{1}{T_f} d\tau \\ &= \int_0^{T_f} \frac{(\lambda'\tau)^\alpha e^{-\lambda'\tau}}{\alpha!} \frac{1}{T_f} d\tau \\ &= \frac{1}{\lambda' T_f \cdot \alpha!} \left\{ \alpha! - e^{-\lambda' T_f} \sum_{i=0}^{\alpha} \frac{\alpha!}{(\alpha - i)!} (\lambda' T_f)^{\alpha - i} \right\}. \end{aligned} \tag{36}$$

The queueing analysis with the presence of cross traffic is generally a difficult task. To simplify the analysis, we assume that during the steady state, the cross traffic arrivals during a slot will not cause the refined Markov chain to deviate from its steady state to a great extent. The performance of the video streaming can be analyzed simply by applying the analysis in Section 3 with modified $P_{\mathcal{B}}$ and $P_{\mathcal{T}}$. Note that $P_{\mathcal{E}}$ is unaffected by the cross traffic.

**Modified Blocking Probability.** The blocking probability with the interruption of cross traffic during the steady state can be written as

$$P_{\mathcal{B}} = \sum_{c \in \Psi, \underline{u} \in \Omega} P(\mathcal{B} | S_{(c,\underline{u})}) \pi_{(c,\underline{u})}, \tag{37}$$

where

$$\begin{aligned} P(\mathcal{B} | S_{(c,\underline{u})}) &= P\{A_c > \max(0, F_{(c,\underline{u})} - N_v)\} \\ &= 1 - \sum_{\alpha=0}^{\beta_{(c,\underline{u})}} P(A_c = \alpha), \end{aligned} \tag{38}$$

with $\beta_{(c,\underline{u})}$ defined as

$$\beta_{(c,\underline{u})} = \max\{0, F_{(c,\underline{u})} - N_v\}. \tag{39}$$

**Modified Timeout Probability.** The modified timeout probability can be expressed as

$$\begin{aligned} P_{\mathcal{T}} &= \sum_{S_{(c,\underline{u})} \in \{S_{(e,\underline{r})} | F_{(e,\underline{r})} > N_v\}} \left\{ \sum_{\alpha \le \max\{0, F_{(c,\underline{u})} - N_v\}} P(\mathcal{T} | S_{(c,\underline{u})}, A_c = \alpha) \right\} \\ &\qquad P(S_{(c,\underline{u})}, A_c = \alpha) \\ &= \sum_{c \in \Psi, \underline{u} \in \Omega'_c} \sum_{\alpha=0}^{\beta_{(c,\underline{u})}} P(\mathcal{T} | S_{(c,\underline{u})}, A_c = \alpha) P(A_c = \alpha) \pi_{(c,\underline{u})}. \end{aligned}$$

Define the number of total packets in the queue including $N_v$ video packets and cross-traffic packets as

$$I_{(c,\underline{u})} = L_{(c,\underline{u})} + N_v + A_c, \tag{40}$$

we can obtain $P(\mathcal{T}|S_{(c,\underline{u})}, A_c = \alpha)$ as

$$P(\mathcal{T}|S_{(c,\underline{u})}, A_c = \alpha) = \sum_{d_1+d_2+\ldots+d_{P-1}<I_{(c,\underline{u})}} P_{c,d_1} P_{d_1,d_2} \cdots P_{d_{P-2},d_{P-1}}. \tag{41}$$

Recall that $P_{d_i,d_k}$ are elements of $\mathbf{P}_c$ in (8).

## 5 Numerical Results

In this section, the numerical experiment results are demonstrated to verify our performance analysis for the video streaming. We consider the transmission of MPEG2 video over wireless LAN. The case of two video streams streaming at the same time is simulated. Both streams have the same content and identical codec setting. The simple MPEG-2 profile is used for video compression, and the codec settings are summarized in Table 2. Note that $N_v(I)$ denotes the number of packets fragmented from I-frame and $N_v(P)$ denotes the number of packets fragmented from P-frame. The simulation parameters of the numerical experiments in this section are summarized in Table 3.

**Table 2.** MPEG-2 codec setting

| Sequence | Foreman |
|---|---|
| Frame rate | 30 frames/sec |
| GOP | 5 |
| Resolution | $176 \times 144$ |
| Chroma format | 4:2:2 |
| Bit-rate | 280kbps , 380kbps |
| $N_v(I)$ | 2 packets , 3 packets respectively |
| $N_v(P)$ | 1 packet |
| Frame pattern | IPPPP |

Figure 7 shows curves of the VFER $\xi(N_v, P_0)$ versus the target PER $P_0$ of the AMC. The solid lines are computed from our analysis whereas the dashed lines are obtained from simulations. One can observe that the proposed analysis is very accurate in capturing the VFER and the tradeoff associated with $P_0$. When the target PER $P_0$ is set too small, the AMC transmits with very low rate. As a results, video packets are queued in the buffer and many of them get expired before transmission. As a result, the VFER is increased. On the other hand, when $P_0$ is very large, though the AMC transmits with high rate which reduces the timeout probability, the PHY errors occur with high probability. As a result, VFER is also increased. Therefore, there is an optimal choice of $P_0$ to minimize the VFER. The star marks in the figure denote the VFER minimum for

**Table 3.** Simulation Parameters

| | |
|---|---|
| Packet size $N_b$ | 1460 bytes |
| Slot duration $T_f$ | 6ms |
| $b$ defined in (2) | 1 |
| The mean of Poisson arrival $\lambda T_f$ | 1 packet/slot |
| Queue size $K$ | 10 packets |
| Nakagami parameter $m$ | 1 (Rayleigh fading) |
| Average SNR $\overline{\gamma}$ | 22 dB |
| Doppler frequency $f_d T_f$ | 0.02 |
| Packet timeout $P$ | 4 slots |
| Target packet error rate $P_0$ | from $10^{-4}$ to $10^{-1}$ |

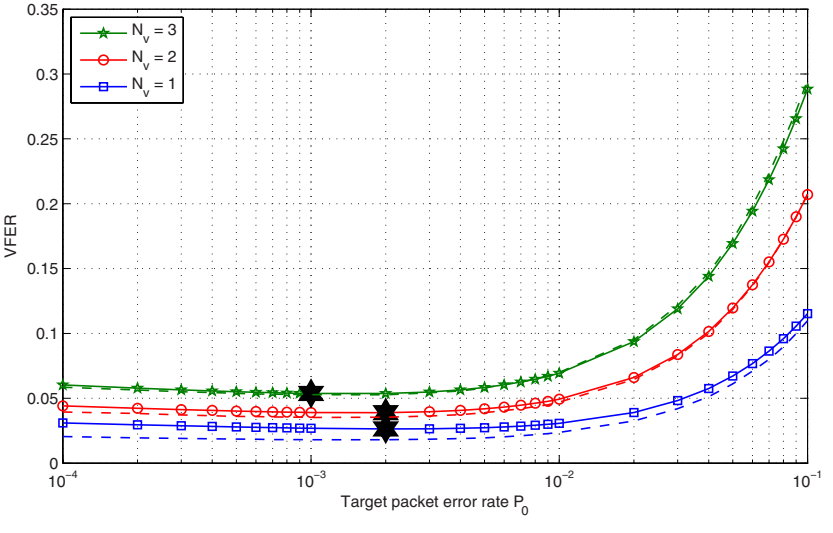


**Fig. 7.** VFER $\xi(N_v, P_0)$ versus $P_0$ with $P = 4$

different values of $N_v$. It is observed that the optimal $P_0$ is different for different $N_v$. To determine the optimal $P_0$ to use, the overall PSNR performance has to be considered.

From the analytical VFER curves of different $N_v$ in Figure 7, the GOP distortion $D_{GOP}(P_0)$ and the resulting PSNR can be computed. The results are illustrate in Figure 8. The dashed lines and the solid lines nearly overlap which indicates our analysis is also accurate in capturing the PSNR performance. From the maximum point of the PSNR curves, we can find the optimal target PER $P_0$ for the video streaming. The SNR thresholds of the AMC can be determined accordingly. Note that the optimal $P_0$ of PSNR is not necessary the same with the optimal $P_0$ of VFER shown in the previous figure.

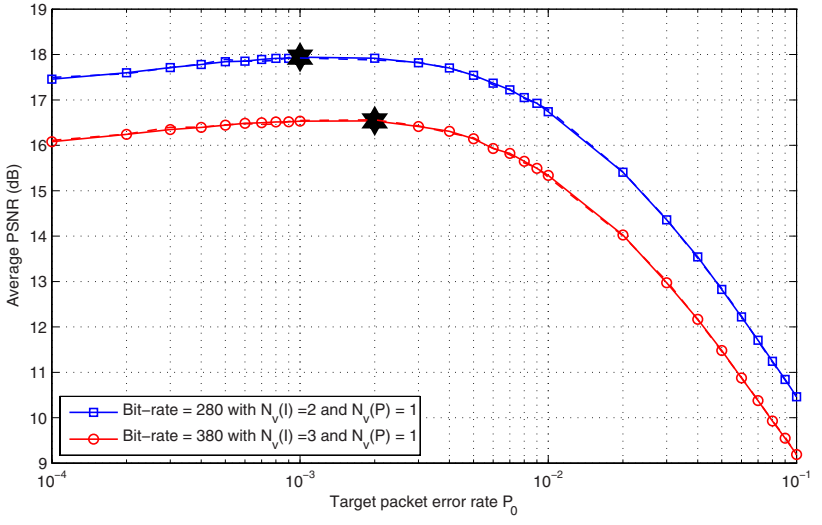


**Fig. 8.** Average PSNR in GOP versus $P_0$ with $P = 4$

## 6 Conclusions

In this paper, an analytical framework has been proposed to analyze the performance of streaming delay sensitive multimedia packets over the wireless fading channel employing the AMC transmission scheme at physical layer. Through the framework, the video frame error rate of video frames of different lengths has been derived. The GOP distortion and the associated PSNR have also been obtained from the video frame error rate. The PSNR can be expressed as a function of the target AMC PER. From the PSNR analysis, one can obtain the optimal target AMC PER to determine the optimal SNR thresholds for the AMC to support multimedia streaming. Simulations show that the proposed analysis is accurate in capturing the performance of the video streaming. It is useful for optimizing the performance of wireless multimedia streaming.

## Acknowledgment

This work was supported in part by the Excellent Research Projects of National Taiwan University under Contract 97R0062-06, by the National Science Council under Contract NSC97-2220-E-002-017, by the Ministration of Education.

## References

1. Liu, Q., Zhou, S., Giannakis, G.B.: Queueing with Adaptive Modulation and Coding over Wireless Links: Cross-layer Analysis and Design. IEEE Trans. Wireless Commun. 4(3), 1142–1153 (2005)

2. Liu, Q., Zhou, S., Giannakis, G.B.: Analyzing and Optimizing Adaptive Modulation Coding Jointly with ARQ for QoS-guaranteed Traffic. IEEE Trans. Veh. Technol. 56(2), 710–720 (2007)
3. Zhou, S., Zhang, K., Niu, Z., Yang, Y.: Queueing Analysis on MIMO Systems with Adaptive Modulation and Coding. In: IEEE Intl. Conf. Commun. (2008)
4. Xu, J., Shen, X., Mark, J.W., Cai, J.: Adaptive Transmission of Multi-layered Video over Wireless Fading Channels. IEEE Trans. Wireless Commun. 6(6), 2305–2314 (2007)
5. Zhang, X., Tang, J., Chen, H., Ci, S., Guizani, M.: Cross-Layer-Based Modeling for Quality of Service Guarantees in Mobile Wireless Networks. IEEE Commun. Mag. (January 2006)
6. Harsini, J., Lahouti, F.: Adaptive Transmission Policy Design for Delay-Sensitive and Bursty Packet Traffic over Wireless Fading Channels. IEEE Trans. Wireless Commun. (2008)
7. Doufexi, A., Armour, S., Butler, M., Nix, A., Bull, D., McGeehan, J.: A Comparison of the HIPERLAN/2 and IEEE 802.11a Wireless LAN Standards. IEEE Commu. Mag. (May 2002)
8. Liu, Q., Zhou, S., Giannakis, G.B.: Cross-layer Combining of Adaptive Modulation and Coding with Truncated ARQ over Wireless Links. IEEE Trans. Wireless Commun. 3(5), 1746–1755 (2004)
9. Molisch, A.: Wireless Communications. John Wiley and Sons, Chichester (2005)
10. Alouini, M., Goldsmith, A.: Adaptive Modulation over Nakagami Fading Channels. Wireless Personal Communications 13, 119–143 (2000)
11. Razavilar, J., Liu, K.J., Marcus, S.: Jointly Optimized Bit-Rate/Delay Control Policy for Wireless Packet Networks with Fading Channels. IEEE Trans. Commun. 50(3), 484–494 (2002)
12. Yacoub, M., Bautista, J., de Rezende Guedes, L.: On Higher Order Statistics of the Nakagami-m Distribution. IEEE Trans. Veh. Technol. 48(3), 790–794 (1999)
13. Chou, P.A., Miao, Z.: Rate-Distortion Optimized Streaming of Packetized Media. IEEE Trans. Multimedia 8(2), 390–404 (2006)